FEMS Microbiology Ecology, 92, 2016, fiw069

doi: 10.1093/femsec/fiw069
Advance Access Publication Date: 31 March 2016
Research Article

RESEARCH ARTICLE

Substrate preference, uptake kinetics and bioenergetics in a facultatively autotrophic, thermoacidophilic crenarchaeote

Matthew R. Urschel[1], Trinity L. Hamilton[2], Eric E. Roden[3,4] and Eric S. Boyd[1,4,*]

[1]Department of Microbiology and Immunology and the Thermal Biology Institute, Montana State University, Bozeman, MT 59717, USA, [2]Department of Biological Sciences, University of Cincinnati, Cincinnati, OH 45221, USA, [3]Department of Geosciences, University of Wisconsin, Madison, WI 53706, USA and [4]NASA Astrobiology Institute, Ames Research Center, Moffett Field, CA 94035, USA

*Corresponding author: Department of Microbiology and Immunology, Montana State University, Bozeman, MT 59717, USA. Tel: 1-406-994-7046; E-mail: eboyd@montana.edu

One sentence summary: Physiological, genomic and bioenergetic characterization of *Thermoproteus* strain CP80 provides new insights into the kinetic and energetic factors that influence the physiology and ecology of facultative autotrophs in high-temperature acidic environments.

Editor: Gary King

ABSTRACT

Facultative autotrophs are abundant components of communities inhabiting geothermal springs. However, the influence of uptake kinetics and energetics on preference for substrates is not well understood in this group of organisms. Here, we report the isolation of a facultatively autotrophic crenarchaeote, strain CP80, from Cinder Pool (CP, 88.7°C, pH 4.0), Yellowstone National Park. The 16S rRNA gene sequence from CP80 is 98.8% identical to that from *Thermoproteus uzonensis* and is identical to the most abundant sequence identified in CP sediments. Strain CP80 reduces elemental sulfur (S_8°) and demonstrates hydrogen (H_2)-dependent autotrophic growth. H_2-dependent autotrophic activity is suppressed by amendment with formate at a concentration in the range of 20–40 μM, similar to the affinity constant determined for formate utilization. Synthesis of a cell during growth with low concentrations of formate required 0.5 μJ compared to 2.5 μJ during autotrophic growth with H_2. These results, coupled to data indicating greater C assimilation efficiency when grown with formate as compared to carbon dioxide, are consistent with preferential use of formate for energetic reasons. Collectively, these results provide new insights into the kinetic and energetic factors that influence the physiology and ecology of facultative autotrophs in high-temperature acidic environments.

Keywords: autotroph; heterotroph; facultative; metabolic switching; Yellowstone; energetics; formate; hydrogen

INTRODUCTION

Facultative autotrophy, or the ability to alter carbon metabolism between the utilization of inorganic (CO_2) and organic sources, has been demonstrated in a number of hyperthermophilic, sulfur-reducing crenarchaeota isolated from high-temperature, sulfur-rich hydrothermal environments (Zillig *et al.* 1981; Huber, Kristjansson and Stetter 1987; Huber *et al.* 2000; Plumb *et al.* 2007; Zillig and Reysenbach 2015). For example, the hyperthermophilic, elemental sulfur (S_8°)-reducing crenarchaeote *Pyrobaculum islandicum* grows autotrophically with hydrogen (H_2)

Received: 14 February 2016; **Accepted:** 28 March 2016

as an electron donor, as well as heterotrophically on complex organic substrates such as peptone, yeast extract, meat extract or cellular homogenate from a variety of bacterial and archaeal cultures (Huber, Kristjansson and Stetter 1987). Likewise, the hyperthermophilic crenarchaeote, *Thermoproteus neutrophilus*, also a sulfur-reducer, grows autotrophically, mixotrophically or heterotrophically (Schäfer, Barkowski and Fuchs 1986; Schäfer *et al.* 1989a,b; Ramos-Vera, Berg and Fuchs 2009; Ra mos-Vera *et al.* 2010).

Organic compounds, including formate, have been reported in the thermal fluids of marine and terrestrial hydrothermal systems in which elemental sulfur is available as an electron acceptor (Rogers and Amend 2005, 2006; Rogers, Amend and Gurrieri 2007; Windman *et al.* 2007; Urschel *et al.* 2015). Previous studies have suggested H_2 as the primary energy source in such environments (Spear, Walker and Pace 2005, 2006) while thermodynamic modeling indicates that the oxidation of organic compounds may yield as much or more energy as the oxidation of H_2 under these conditions (Amend *et al.* 2003; Rogers and Amend 2006; Windman *et al.* 2007). This suggests that microorganisms in these hydrothermal environments may grow heterotrophically as opposed to autotrophically using H_2 when suitable organic substrates are available. Recent studies provide some evidence for this. For example, *T. neutrophilus* was shown to preferentially utilize organic carbon substrates over CO_2, when both were available (Schäfer, Barkowski and Fuchs 1986; Schäfer *et al.* 1989a,b; Ramos-Vera, Berg and Fuchs 2009; Ramos-Vera *et al.* 2010). Moreover, the generation times of S_8°-reducing *T. neutrophilus* cultures growing mixotrophically with acetate, 4-hydroxybutyrate, succinate or pyruvate were up to 66% shorter than those exhibited in cultures growing autotrophically with H_2 and CO_2 (Ramos-Vera *et al.* 2010). Under these mixotrophic growth conditions, a significant percentage of the carbon incorporated into biomass came from organic substrates, rather than CO_2, leading to the conclusion that cells were downregulating CO_2 assimilation to allow for the preferential use of carbon from organic acids.

We recently demonstrated CO_2 and formate assimilation in 13 geochemically distinct, high-temperature (>73°C) hot springs in Yellowstone National Park (YNP) using a microcosm-based approach (Urschel *et al.* 2015). In that study, amendment of microcosms with low concentrations of formate (<20 μM) suppressed CO_2 assimilation, even over short (<60 min) incubation times. The observed suppression of CO_2 assimilation by amendment with low concentrations of formate over such a short timeframe suggested that the same populations were involved in both CO_2 fixation and formate oxidation in these hot springs. These results indicate that facultative autotrophs alter their metabolism to preferentially utilize the more thermodynamically favorable (and reduced) substrate formate (Urschel *et al.* 2015), when both substrates are available. Indeed, kinetic experiments indicated that the formate-utilizing populations in these geothermal springs were adapted to utilize formate at low concentration with measured community uptake affinity constants (K_s) ranging from 2.3 to 36.9 μM, which largely corresponded with the concentrations of formate required to suppress autotrophic activity in these communities.

The dominant 16S rRNA gene sequences identified in hot springs where our previous microcosm-based experiments were conducted were often closely affiliated with facultative autotrophs or with organisms whose genome sequences suggest a facultatively autotrophic lifestyle (Urschel *et al.* 2015). For example, the dominant archaeal 16S rRNA gene sequence identified in sediments sampled from Cinder Pool (CP, 88.7°C, pH 4.0), YNP was closely affiliated (98.8% sequence identity) with *T. uzonensis* 768-20, which was isolated from a hot spring in Russia (Bonch-Osmolovskaya *et al.* 1990).

The genus *Thermoproteus* includes strains with a wide range of metabolic strategies including obligate heterotrophy, obligate autotrophy, mixotrophy and facultative autotrophy. For example, *T. tenax* is capable of growth with H_2 and CO_2 alone (Fischer *et al.* 1983), or with organic substrates including glucose, casamino acids, ethanol, malate or formamide as the sole carbon and electron source (Zillig *et al.* 1981; Selig and Schönheit 1994). *Thermoproteus neutrophilus* can grow autotrophically, mixotrophically or heterotrophically using acetate, 4-hydroxybutyrate, succinate and pyruvate (Schäfer, Barkowski and Fuchs 1986; Schäfer *et al.* 1989a,b; Ramos-Vera, Berg and Fuchs 2009; Ramos-Vera *et al.* 2010). In contrast, *T. uzonensis* grows via the fermentation of complex organic carbon such as peptone or tryptone while growth is not supported by more simple organic compounds. Neither autotrophic growth nor growth on formate has been demonstrated in pure cultures of *T. uzonensis* (Bonch-Osmolovskaya *et al.* 1990) despite the presence of genes encoding an archaeal-type formate dehydrogenase (FDH) and a complete dicarboxylate/4-hydroxybutyrate pathway in the genome (Huber *et al.* 2008; Mardanov *et al.* 2011). This suggests the potential for heterotrophic use of formate or autotrophic CO_2 assimilation and implies that *T. uzonensis* may be a facultative autotroph.

Here we aimed to investigate the substrate preference, uptake kinetics and energetics of facultative autotrophs in geothermal systems. Our efforts focused on CP since this YNP hot spring has been shown to harbor abundant 16S rRNA gene sequences closely affiliated with the putative facultative autotroph, *T. uzonensis*, and autotrophic activity in this spring was shown to be suppressed by low (~20 μM) concentrations of formate (Urschel *et al.* 2015). Moreover, unlike a variety of other springs in YNP (Windman *et al.* 2007; Urschel *et al.* 2015) the concentration of formate in CP was shown to be below the limits of detection (<100 nM) (Urschel *et al.* 2015) which may indicate that this substrate is used as quickly as it is produced/introduced into the system. An important consideration for this study is that formate, like other organic acids, becomes increasingly cytotoxic with decreasing pH (Pronk *et al.* 1991). Cytotoxicity results from the ability of an organic acid, when protonated and uncharged, to readily diffuse into the cell and deprotonate at intracellular pH, thereby decreasing the membrane potential and decoupling ion translocation from ATP production (Russell 1992). The percentage of the total amount of an organic acid that is protonated at any given pH is directly proportional to its pKa, making organic acids with a higher pKa potentially more cytotoxic than those with a lower pKa in acidic environments such as CP. For instance, the pKa of formate is 3.75 at 80°C (Amend and Shock 2001), indicating that half of the available formate pool is protonated and uncharged at this pH and capable of diffusion into the cell.

In this study, we employed an enrichment strategy targeted toward organisms that could utilize formate but also designed to avoid formate cytotoxicity by maintaining concentrations between ~30 and 100 μM. As a result, we isolated a crenarchaeote (strain CP80) capable of formate-dependent or hydrogen-dependent growth, with S_8° as the electron acceptor. The partial 16S rRNA gene sequence from the genome of CP80 exhibited 98.8% sequence identity with the 16S rRNA gene from *T. uzonensis* and was identical to the dominant archaeal 16S rRNA gene sequence present in sediments sampled from CP (Urschel *et al.* 2015). Here we present physiological, kinetic,

energetic and genomic data generated from studies of strain CP80 to further elucidate the physiological mechanisms that influence the shift between formate-dependent heterotrophic and hydrogen-dependent autotrophic growth. Comparison of these results to cultivars with available genomic data suggests that facultative autotrophy and preferential utilization of organic acids may be a widespread metabolic strategy employed by a diversity of S_8°-dependent crenarchaeotes that commonly inhabit high-temperature hydrothermal systems.

MATERIALS AND METHODS

Physical and chemical measurements

Field sampling and measurements were conducted at CP (N 44°43′56.8″, W 110°42′35.1″), in Norris Geyser Basin, YNP, Wyoming on 31 May 2012. The pH, temperature and conductivity of spring waters were measured on site with a temperature compensated YSI pH100CC-01 pH meter and a YSI EC300 conductivity meter (YSI, Inc., USA), respectively. Ferrous iron (Fe^{2+}) and total sulfide (S^{2-}) concentrations in CP were quantified using Hach ferrozine pillows and Hach sulfide reagents 1 and 2, respectively, and a Hach DR/890 field portable spectrophotometer (Hach Company, Loveland, CO). Detection limits of Hach kits are 0.2 μM and 0.3 μM for Fe^{2+} and S^{2-}, respectively. Precision of Hach kits are $\pm$0.07 μM and $\pm$ 0.63 μM for Fe^{2+} and S^{2-}, respectively.

Enrichment and isolation of strain CP80

Clay-rich sediments were sampled aseptically from CP with a flame-sterilized spatula, placed in a sterile serum bottle, and overlaid with a small amount (~5 mL) of unfiltered spring water. Serum bottles and their contents were capped with a butyl rubber stopper and an aluminum crimp seal, briefly purged with N_2, and stored in a thermos filled with spring water (to minimize temperature change) during transport back to the lab at MSU. Samples were stored in an incubator at 80°C for $\leq$24 h before being used for enrichment and isolation.

A previously described base salts enrichment medium (Boyd *et al.* 2007) consisting of $MgSO_4$ (0.33 g L^{-1}), NH_4Cl (0.33 g L^{-1}), $CaCl_2$ (0.33 g L^{-1}), KCl (0.33 g L^{-1}) and KH_2PO_4 (0.33 g L^{-1}) was prepared for use in enrichment and isolation of organisms capable of growth on formate (added to a final concentration of 50 μM) as the sole carbon and electron source. The pH of the medium was adjusted to 4.0 with concentrated hydrochloric acid and 35 mL of base salts medium was dispensed into several 70 mL serum bottles. Serum bottles and their contents were purged for $\geq$45 min with nitrogen (N_2) gas passed over heated (210°C) and H_2-reduced copper shavings to remove oxygen, capped with butyl rubber septa, and autoclave sterilized. Following sterilization, orthorhombic elemental sulfur flower (S_8°; 5 g L^{-1}, autoclaved dry under an N_2 atmosphere at 110°C for 1 h) was added to each serum bottle under a stream of sterile N_2 gas. Finally, filter-sterilized and anoxic (N_2 purged) SL-10 trace elements and Wolfe's vitamins were added to a final concentration of 1 mL L^{-1} as previously described (Boyd *et al.* 2007). For simplicity, this medium will be referred to as S_8°-base salts for the remainder of this communication.

S_8°-base salts medium was inoculated with 100 μL of the sediment/water slurry collected from CP, and the cultures were incubated at 80°C. Cultures were amended with an additional 50 μM formate every 72 h from a sterile, anaerobic stock solution prepared in S_8°-base salts medium at pH 4.0. S_8° reduction activity in cultures was monitored by measurement of the production of total sulfide, as determined via the methylene blue method (Fogo and Popowsky 1949). Cultures exhibiting significantly greater sulfide production activity than that observed in uninoculated controls were used in a subsequent dilution to extinction cultivation assay aimed at obtaining a pure culture. Briefly, a series of eight 125 mL serum bottles were prepared with 45 mL of S_8°-base salts medium amended with formate to a final concentration of 50 μM. S_8°-base salts medium was inoculated with 5 mL of inoculum taken from enrichment cultures exhibiting sulfide production activity, for an initial dilution factor of 10^{-1}. A 10-fold dilution to extinction isolation strategy was employed from this first dilution to a final dilution factor of 10^{-8}. Cultures were incubated at 80°C for ~7 days, followed by the inoculation of a newly prepared dilution series from the most dilute culture group showing S_8° reduction activity in the previous dilution series. Progress toward enrichment of a population with a single morphotype was monitored in each dilution to extinction culture series by epifluorescence microscopy using SYBR Gold Nucleic Acid Gel Stain (Life Technologies, Inc., Grand Island, NY) as previously described (Boyd *et al.* 2007). A separate series of serum bottles containing S_8°-base salts were prepared for use in monitoring abiotic production of sulfide.

Genomic characterization of strain CP80

Following four rounds of dilution to extinction, a single morphotype was observed. Three 5 mL subsamples of a culture with this single morphotype were harvested via centrifugation (14 000 × g, 15 min, 4°C), and total DNA was isolated from the cell pellets using the FastDNA Spin Kit for soils (MP Biomedicals, Santa Ana, CA). Equal volumes of replicate extractions were pooled and quantified using the Qubit DNA Assay kit and a Qubit 2.0 Fluorometer (Life Technologies). A total of 35 cycles of PCR were conducted using bacterial- (1100F/1492R) or archaeal-specific (344F/915R) 16S rRNA gene primers with reaction and cycling conditions as previously described (Hamilton *et al.* 2013). Amplicons were not generated using bacterial-specific PCR primers. The archaeal 16S rRNA gene amplicons were subjected to paired-end Illumina MiSeq sequencing (Illumina, San Diego, CA). Post-sequencing processing was performed with Mothur (Schloss *et al.* 2009) as previously described (Hamilton *et al.* 2013) after removing reads of less than 300 base pairs (bp). The NCBI SRA accession number for raw 16S rRNA gene sequence and quality files is SRR1812888.

Total genomic DNA was sequenced at the Genomics Core Facility at the University of Wisconsin-Madison using the paired-end Illumina MiSeq platform. DNA fragments were prepared according to the manufacturer's protocol. Quality of the reads was checked with FastQC (bioinformatics.babraham.ac.uk/projects/fastqc). Reads were quality trimmed from both ends using Trimmomatic (Bolger, Lohse and Usadel 2014). Reads containing more than three N's were removed and reads with an average quality score of less than Q20 or a sequence length less than 50 bp were removed. The trimmed paired-end reads were assembled using SPAdes version 3.5.0 (Nurk *et al.* 2013) and were annotated using the RAST server (Aziz *et al.* 2008). A draft genome was assigned to the taxon *Thermoproteales* using the taxonomic affiliation of predicted genes based on the best BLASTx match. The NCBI SRA database accession number for raw paired-end metagenomic sequence files is SRR1812888. The DDBJ/EMBL/GenBank accession number for this partial genome shotgun project is LCWM00000000.

S_8°-dependent growth of strain CP80 on formate or H_2/CO_2

Strain CP80 was grown in S_8°-base salts medium with formate as the sole carbon source and electron donor or CO_2 as carbon source with H_2 as the electron donor. Triplicate cultures were prepared for both biological and abiological (uninoculated) incubations as described above with the following exception for cells grown on 20% CO_2/ 80% H_2: the N_2 headspace was purged for 1 min with sterile H_2 passed over heated (210°C) copper shavings. Stock solutions (10 mM) containing a 170:1 ratio of ^{12}C to ^{14}C formate or bicarbonate were used to amend media with 50 μM formate or bicarbonate. Given that the pKa for bicarbonate/$CO_{2(aq)}$ at 80°C is ~6.4 (Amend and Shock 2001), it was assumed that the added bicarbonate completely dissociated to CO_2 when added to S_8°-base salts medium with the pH adjusted to 4.0 and equilibrated with headspace CO_2.

Formate or H_2/CO_2-amended cultures were inoculated to an initial cell density of 10^5 to 10^6 cells mL^{-1} from mid-log phase stock cultures grown on formate/S_8° or $H_2/CO_2/S_8^\circ$, respectively. All cultures were incubated at 80°C for the duration of the experiment. Subsamples were collected from cultures every 24 to 48 h for determination of cell concentrations and determination of oxidation or assimilation of formate or CO_2 (described below). The concentration of total sulfide was measured in each culture for each time point. Total sulfide concentration was determined by summing the concentrations of gaseous sulfide and aqueous sulfide in each culture (as calculated using Henry's Law; Sander 2014). Cell counts were performed using epifluorescence microscopy as described above. Cell counts could not be normalized to units of cell mass due to low cell densities and our inability to measure protein using a variety of methods (data not shown). Since cultures did not enter exponential growth phase due to limited nutrient availability, generation times (T_n) were calculated based on cell densities at time points comprising the steepest portion of the observed growth curves. Thus, T_n, as reported for this set of experiments, may underestimate true T_n.

Rates of substrate transformation

N_2-purged serum bottles (12 mL) containing 1 mL of the CO_2-absorbing solution Carbo-Sorb® E (PerkinElmer, Inc., Santa Clara, CA, USA) were evacuated to a final pressure of –1.3 kPa using a vacuum pump for use in determining the concentration of CO_2 produced in the gas phase of cultures grown on formate. A total of 1 mL of the gas phase was removed from the headspace of each culture using a 1 mL syringe and stopcock and immediately injected into one of the bottles containing Carbo-Sorb E solution.

To determine the concentration of dissolved CO_2 produced during growth on formate, 2 mL of culture was removed from each microcosm and injected into a 12 mL serum bottle prepared as described above, but without Carbo-Sorb E solution. The sealed 2 mL subsamples were acidified by the addition of 0.2 mL 12N hydrochloric acid to ensure that the concentration of inorganic carbon remaining in the solution was minimized. Following 2 h equilibration, 5 mL of the headspace (at atm pressure) were removed using a 10 mL syringe and stopcock and injected into a separate 12 mL serum bottle containing 1 mL Carbo-Sorb E solution, prepared as described above. Serum bottles containing gas samples and Carbo-Sorb E solution were allowed to react at room temperature (~22°C) for approximately 2 h. Following incubation, the vials were opened and the Carbo-Sorb E solution was removed and transferred to a 20 mL liquid scintillation vial containing 10 mL CytoScint ES liquid scintillation fluid (MP Biomedicals) in preparation for liquid scintillation counting (LSC), as described below.

The amount of ^{14}C assimilated during growth of strain CP80 on either formate or CO_2 was determined by removal of 2 mL subsamples from each culture. Samples were acidified as described above and filtered onto sterile, white 0.22 μm polycarbonate membranes. Filtered samples were washed with 5 mL of culture medium (pH 4.0, no carbon source), dried for 1–2 h at 80°C, placed in scintillation vials and overlaid with 10 mL of CytoScint ES liquid scintillation fluid. Radioactivity associated with each of the samples (Carbo-Sorb E solution and filtered biomass) was measured on a Beckman LS 6500 LSC (Beckman Coulter, Inc., Indianapolis, IN) with an estimated detection limit of 30 and 32 pM for ^{14}C-formate and bicarbonate, respectively. Detection limits were based on the known background counts associated with this scintillation counter and the specific activity of the radiolabeled substrates used. Rates of oxidation (i.e. mineralization) and/or assimilation of formate and CO_2 were calculated from liquid scintillation counts using previously described methods (Urschel *et al*. 2015). The mean and standard error of the rates of substrate transformation attributable to biological activity was calculated as the difference between substrate transformation rates in three biological replicates and three abiological (uninoculated) controls. The amount of formate remaining in culture medium (residual formate) was determined by mass balance.

Suppression of CO_2 assimilation by formate

Serum bottles (70 mL) containing 10 mL of S_8°-base salts medium were prepared as described above. Following removal of O_2 via N_2 sparging, the headspace of each culture was purged for 1 min with filter sterilized (passed through 0.22 μm filters) H_2 followed by the addition of CO_2 to achieve a final concentration of 20% CO_2 to 80% H_2. A total of 5 μCi (0.1 μmol) of ^{14}C-bicarbonate was added to the culture medium. The culture medium was then amended with 0, 5, 10, 20, 40 or 80 μM ^{12}C-formate. Cultures were inoculated from H_2/CO_2 grown log phase cultures to an initial cell density of 10^6 cells mL^{-1}. Following 4 h incubation at 80°C, S_8°-base salts medium was acidified to a pH < 2.0 as described above to volatilize unreacted $^{14}CO_2$. Bottles were allowed to degas for 1 h in a fume hood followed by filtration of cells onto 0.2 μm white polycarbonate membrane filters. Membranes were dried at 80°C for 24 h, and the ^{14}C activity in the biomass of each culture was determined by LSC as described above. The percent suppression of CO_2 assimilation activity at each formate concentration was determined by normalization of the ^{14}C activity in the biomass of the formate-amended cultures to that in the unamended cultures.

Kinetics of formate conversion

Serum bottles (125 mL) containing 50 mL S_8°-base salts medium were amended with 10 mM ^{12}C+^{14}C-formate stock solution (prepared as described above) to achieve a final formate concentration of 1.25, 2.50, 5.00, 10.0, 20.0 or 40.0 μM. Cells for use as inoculum were prepared by filtration of 50 mL of mid-log phase formate-grown cultures onto a sterile 0.2 μm polycarbonate filter. Filtered cells were washed with 20 mL of base salts medium (pH 4.0) lacking S_8° and a carbon source to remove residual formate that might be carried over from the inoculum. Filtered cells were resuspended in 20 mL sterile base salts medium (pH 4.0) lacking S_8° and a carbon source, and 1 mL of this inoculum

was added to each microcosm to achieve an initial cell density of ~10^5 cells mL^{-1}. Cultures were incubated at 80°C for 24 h, and subsamples of the gas and aqueous phases of cultures were taken at intervals of 8 h as described above. The amount of CO_2 produced via formate oxidation was calculated by summing the aqueous and gas phase CO_2 concentrations determined by liquid scintillation counts as described above. The Michaelis constant (K_s) of formate conversion to CO_2 was estimated from a plot of the formate conversion rate during log phase growth versus substrate concentration using the KaleidaGraph software package (Synergy Software, Reading, PA, USA). Reported values reflect the average and standard error of measurement of three replicate biological cultures minus values from three replicate abiological cultures.

Cell yields of strain CP80 when grown on formate and H_2/CO_2

The coupling of formate ($HCOO^-$) or H_2 oxidation with the reduction of S_8° (simplified to indicate reduction of a single atom of S°) should follow the reaction stoichiometry as depicted in equations 1 and 2 below, respectively:

$$S^\circ + HCOO^- (aq) + H_2O \Rightarrow H_2S (g) + HCO_3^- (aq) \quad (1)$$

$$H_2 (g) + S^\circ \Rightarrow H_2S (g) \quad (2)$$

The ratio of total formate transformed to total S_8° reduced was determined by dividing the amount of formate transformed by the amount of S_8° reduced (derived from total sulfide produced) at each time point, followed by calculation of the mean and standard error of measurement of this ratio across all time points. H_2 concentration was not monitored during growth and thus the ratio of total H_2 oxidized to total S_8° reduced could not be calculated. The amount of carbon assimilated per cell (fmol C assimilated $cell^{-1}$) during growth on formate or CO_2 was calculated by dividing the total C assimilated from formate or CO_2 at each time point by the number of new cells produced at each time point. This was followed by calculation of the mean and standard error of measurement of these ratios across all time points.

The total amount of energy available to an organism catalyzing a redox reaction in a non-standard state displaced from equilibrium is given by equation 3:

$$\Delta_r G = \Delta_r G^\circ + RT \ln Q_r, \quad (3)$$

where $\Delta_r G$ is the Gibbs free energy of reaction, $\Delta_r G^\circ$ is the standard Gibbs free energy of reaction, R is the ideal gas constant (~8.314 J mol^{-1} K^{-1}), T is the temperature in Kelvin (K) and Q_r is the activity product (the product of the activities of each reactant and product, where reactant activities are negative, and product activities are positive). The activity (α) of each reactant and product can be calculated from its aqueous concentration and the ionic strength of the aqueous solution in which the reaction proceeds using the extended Debye–Hückel equation (Helgeson 1981).

Reactant and product activities at each sampling time during growth of strain CP80 on formate and H_2/CO_2 were calculated based on the ionic strength and composition of the S_8°-base salts medium as described above, as well as the measured or estimated concentration of each reactant and product, using the freeware chemical equilibrium modeling application Visual MINTEQ 3.0. Reactant and product activities were then used to compute $\Delta_r G^\circ$ and ln Q_r using the *subcrt* command in the thermodynamic modeling package CHNOSZ (Dick 2008), developed for use with the statistical computing language R (Team 2012). Calculated $\Delta_r G^\circ$ and ln Q_r values were then used to calculate $\Delta_r G$ with equation 3 above, and the resulting $\Delta_r G$ value was divided by the total number of electrons transferred per mol substrate transformed to determine the energy available per mol electron transferred (kJ mol e^{-1}). At each time point, the energy available to cultures of CP80 was calculated from the Gibbs energy calculations, as described above, and the total number of electrons transferred from the reductant to the oxidant at that time point was calculated. The total energy available from the individual catalyzed redox reaction at each time point was divided by the total amount of carbon assimilated at that time point to compute the amount of energy required to assimilate carbon. Similarly, the total energy available from the individual catalyzed redox reaction at each time point was then divided by the number of new cells produced at each time point to compute the amount of energy required to produce a single cell. Since we did not quantify differences in H_2 concentration during the growth of strain CP80, we assumed a constant aqueous H_2 concentration equal to the saturation concentration of H_2 in H_2O at 80°C and 1 atm of partial pressure (~768 μM) for these calculations.

RESULTS

Site description

CP is a high-temperature, acid-sulfate-chloride hot spring located in Norris Geyser Basin, YNP. We have observed the temperature and pH of the spring to be fairly constant, ranging from 84°C to 89°C and 4.0 to 4.4, respectively, over the past 12 years of sampling (data not shown). These pH and temperature range are similar to the historical average for CP (White, Hutchinson and Keith 1988). CP is a unique feature in YNP in that a reservoir of molten S_8° is present at a depth of ~18 m, while its surface is partially covered with black, hollow spherules comprised of ~99.0% S_8° and ~1.0% pyrite (White, Hutchinson and Keith 1988). At the time when samples were collected for enrichment and isolation of strain CP80, the temperature, pH and conductivity in CP source waters were 88.7°C, 4.0 and 4.8 mS, respectively. Total sulfide and ferrous iron concentrations at the site at this time were 6.2 and 4.2 μM, respectively.

Enrichment and isolation of strain CP80

Clay-rich sediment collected from the edge of CP was used to inoculate S_8°-base salts media containing 50 μM formate as the sole carbon and energy source. Incubation of the cultures at 80°C resulted in sulfide formation within 5 days, indicating S_8° reduction activity. Four successive rounds of dilution to extinction cultivation (10-fold dilutions to a final dilution of 10^{-8}) resulted in the isolation of a single morphotype, designated as strain CP80. Further confirmation of the purity of the final CP80 dilution to extinction culture was checked by PCR amplification and Illumina sequencing of the 16S rRNA genes in DNA extracted from these cultures. The 16S rRNA gene from the genome of CP80 was closely affiliated (98.8% sequence identity) with *T. uzoniensis* 768-20 within the crenarchaeal order *Thermoproteales*, and was 100% identical to the dominant archaeal 16S rRNA gene sequence that was obtained in our previous characterization of 16S rRNA gene

diversity at CP (Urschel *et al.* 2015). For the remainder of this communication, the strain will be referred to as *Thermoproteus* sp. CP80 or as strain CP80. The rate of sulfide production by CP80 was highest at pH 4.0 suggesting that this is the pH of optimal growth (Fig. S1, Supporting Information). As a result, all subsequent experiments were conducted in medium with the pH adjusted to 4.0.

Growth parameters of *Thermoproteus* sp. CP80 on formate

When grown on formate and S_8°, the generation time (T_n) of strain CP80 was 33.9 ± 2.1 h (Fig. 1A, Table 1). The rate of formate mineralization and assimilation during log phase growth was 20.4 ± 7.2 nmol μg C^{-1} h^{-1} and 1.0 ± 0.3 nmol μg C^{-1} h^{-1}, respectively. The maximum rate of S_8° reduction, as assessed by total S^{2-} production, was 31.9 ± 8.9 nmol μg C^{-1} h^{-1}. The ratio of total formate transformed to total S_8° reduced was 0.8 ± 0.2 nmol μg C^{-1} h^{-1}, which is not statistically different from the expected 1:1 molar ratio of formate oxidized to S_8° reduced (equation 1). Formate mineralization and assimilation activity decreased as the remaining formate concentration approached ~30 μM (Fig. 1B). At this point, the rate of S_8° reduction decreased substantially (Fig. 1C). When additional formate was added at 168 h (final concentration 65 μM), the rate of formate transformation increased to 9.3 ± 3.7 nmol μg C^{-1} h^{-1} which was ~46% of the observed maximum formate transformation rate. A concomitant increase in S_8° reduction activity was observed upon amendment with additional formate (Fig. 1C), with production of sulfide ceasing when formate oxidation ceased (Fig. 1B). The estimated biomass yield was 99.3 ± 31.1 fmol C assimilated $cell^{-1}$. The amount of C assimilated per unit energy conserved from formate/S_8° (equation 1) was 209.2 ± 28.4 fmol C μJ^{-1}, while the amount of energy required to synthesize a cell under these conditions was 0.5 ± 0.2 μJ $cell^{-1}$ (Table 2).

Growth parameters of *Thermoproteus* sp. CP80 on H_2 and CO_2

When CP80 cells were grown autotrophically with H_2 and S_8° (Fig. 2), the T_n was 85.5 ± 4.7 h, which is roughly 2.5-fold longer than when grown on formate and S_8°. Moreover, a lag phase of 96 h was observed which is roughly 4-fold longer than the lag phase of CP80 cells when grown with formate (data not shown). This lag phase was observed when cells used as inoculum were grown with formate or with H_2 and CO_2. The maximum rate of C assimilation from CO_2 was 0.2 ± 0.1 nmol μg C^{-1} h^{-1}, which is significantly lower than the maximum rate of C assimilation observed when cells of CP80 were grown on formate (1.0 ± 0.3 nmol μg C^{-1} h^{-1}) (Table 1). The maximum rate of S_8° reduction, as assessed by sulfide production, was 55.4 ± 9.1 nmol μg C^{-1} h^{-1}. The biomass yield was 46.5 ± 30.0 fmol C $cell^{-1}$, which was not significantly different from that observed in CP80 grown on formate (99.3 ± 31.1 fmol C $cell^{-1}$) (Table 2). This is consistent with microscopic evidence indicating that the cells were of about the same size when grown in the different medium compositions (data not shown). The amount of C assimilated per unit energy conserved from on H_2/S_8° (equation 2) was 19.0 ± 0.3 fmol C μJ^{-1} which was 9.1% of that calculated when cells were grown with formate. The amount of energy required to synthesize a cell under H_2/CO_2-dependent conditions was 2.5 ± 1.6 μJ $cell^{-1}$ which is a factor of 5 greater than that (0.5 ± 0.2 μJ $cell^{-1}$) under formate-dependent conditions (Table 2).

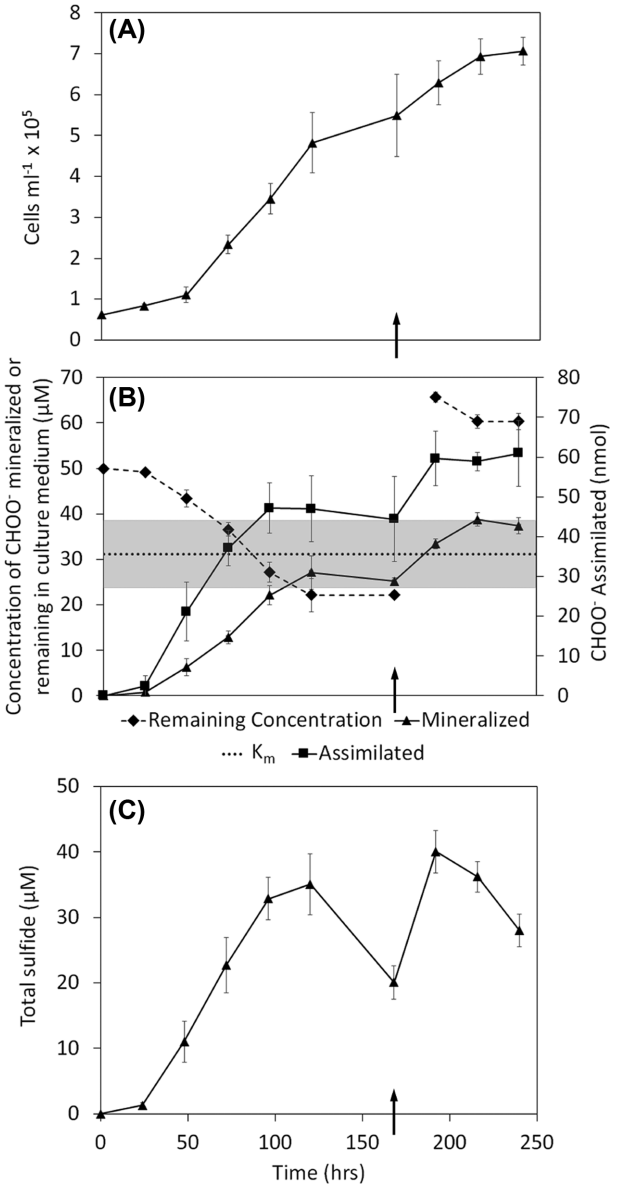

Figure 1. Concentration of cells (**A**), concentrations of formate oxidized (as determined from CO_2 produced), formate assimilated (i.e. incorporated into biomass) and formate remaining in culture medium (**B**), and sulfide produced (**C**) by *Thermoproteus* sp. CP80 incubated at 80°C in S_8° base salts medium (pH 4.0) with formate and S_8° as the sole electron donor and electron acceptor, respectively. The gray box in panel B delineates the average (line in center of box; 31.2 μM) and standard error (half of the width of box; 7.3 μM) of replicate determinations of the K_m (31.2 ± 7.3 μM) for formate transformation (see Fig. 3). Arrows indicate the time point at which cultures were amended with additional formate (50 μmol L^{-1}). The average and standard error of measurement (SEM) of three replicate cultures is presented for each data point.

Formate transformation kinetics and substrate preference in *Thermoproteus* sp. CP80

The rate of CO_2 assimilation in CP80 cultures grown on $H_2/CO_2/S^\circ$ was not significantly suppressed in the presence of 5 or 10 μM formate when compared to that of the unamended control (0 μM formate), but decreased by approximately 22% in the presence of 20 μM formate and was below the limits of detection in the presence of 40 and 80 μM formate (Fig. 3A). Using

Table 1. Generation times and substrate utilization rates by *Thermoproteus* sp. CP80 during incubation at 80°C in S_8°-base salts medium (pH 4.0) with formate or H_2/CO_2 as sole carbon source and S_8° as sole electron acceptor. Rates are normalized to total C assimilated from either formate or CO_2. Units are nmol μg C^{-1} h^{-1}.

Substrate	T_n (h)	Max. substrate oxidation rate	Max. rate of C assimilation	Max. S_8° reduction rate
Formate	33.9 ± 2.1	20.4 ± 7.2	1.0 ± 0.3	31.9 ± 8.9
CO_2/H_2	85.5 ± 4.7	ND	0.2 ± 0.1	55.4 ± 9.1

Max., maximum; ND, no data.
Error reported as standard deviation.

Table 2. Reaction stoichiometries, cell yields, and energetics of *Thermoproteus* sp. CP80 incubated at 80°C in S_8°-base salts medium (pH 4.0) with formate or H_2/CO_2 as sole carbon/energy source and S_8° as sole electron acceptor. The ΔG_r at time 0 h for formate and H_2/CO_2 growth conditions were –122 and –77.0 kJ mol e^{-1}, respectively (see Fig. S2, Supporting Information).

	Yields		
Redox reaction	fmol C Assimilated $cell^{-1}$	fmol C Assimilated μJ^{-1}	μJ $cell^{-1}$
$S_{(s)} + HCO_2^-{}_{(aq)} + H_2O_{(l)} \rightarrow H_2S_{(g)} + HCO_3^-{}_{(aq)}$	99.3 ± 31.1	209 ± 28.4	0.5 ± 0.2
$H_{2\,(g)} + S_{(s)} \rightarrow H_2S_{(aq)}$	46.5 ± 30.0	19.0 ± 0.30	2.5 ± 1.6

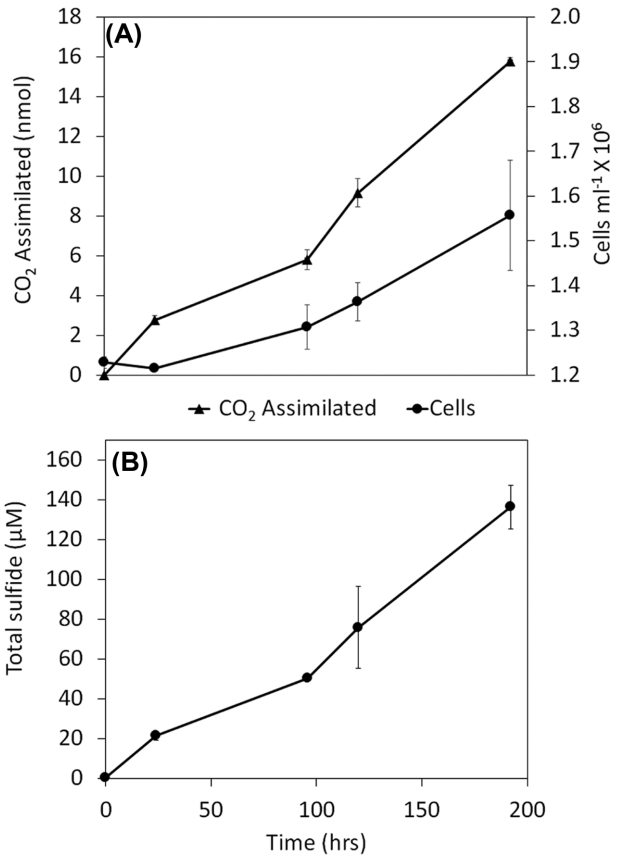

Figure 2. Concentration of cells and the amount of carbon assimilated from CO_2 (**A**), and total sulfide produced (**B**), by *Thermoproteus* sp. CP80 during incubation at 80°C and in S_8° base salts medium (pH 4.0) with CO_2 as the sole carbon source, hydrogen (H_2) as the sole electron donor and S_8° as the sole electron acceptor. The average and standard error of measurement of three replicate cultures is presented for each data point.

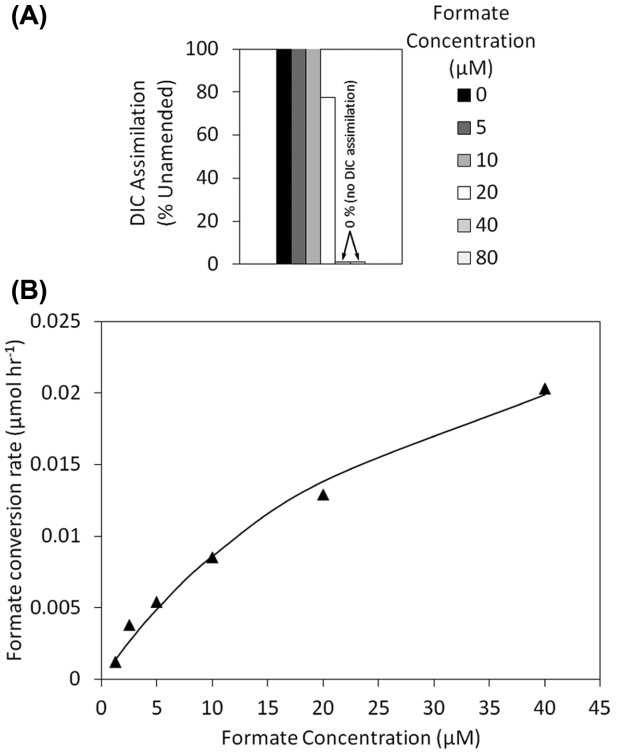

Figure 3. (**A**) Suppression of DIC assimilation in cultures of *Thermoproteus* sp. CP80 incubated at 80°C in S_8° base salts medium (pH 4.0) amended with 0, 5, 10, 20, 40 or 80 μM formate. The data presented reflect the average of three replicate cultures. (**B**) Formate conversion rate by *Thermoproteus* sp. CP80 incubated at 80°C in S_8° base salts medium (pH 4.0) plotted as a function of formate concentration. $K_m = 31.2 \pm 7.3\,\mu$M, $V_{max} = 0.036 \pm 0.005\,\mu$mol h^{-1}, $\chi^2 = 2.71 \times 10^{-6}$, R = 0.99. The data presented reflect the average of three replicate cultures (standard error is not presented).

Henry's Law:

$$[^{12}CO_{2(aq)}] = P^i/K_H,$$

where P^i is the partial pressure of $^{12}CO_2$ in the headspace (0.2 atm at 20% $^{12}CO_2$) and K_H is the Henry's Law constant for CO_2 (29.41 atm M^{-1}), the aqueous concentration of $^{12}CO_2$ in these cultures is calculated to be 6.8 mM. The addition of 1 μmol of $H^{14}CO_3$ to 10 mL of culture media results in a final $H^{14}CO_3$ concentration of 0.1 mM, which gives a ^{14}C:^{12}C ratio of 0.0147. Even in the event that the maximum of 80 μM ^{12}C-formate was oxidized to 80 μM $^{12}CO_{2(aq)}$, this would result in a $^{12}CO_2$ concentration of 6.88 mM, which gives a new ^{14}C:^{12}C ratio of 0.0145, which is a decrease in ^{14}C:^{12}C ratio of only 1.2%. Therefore, the concentration of ^{14}C-formate (a maximum of 80 μM) added to the cultures in which CO_2 assimilation was suppressed was not sufficient to dilute the ^{14}C pool enough to account for this suppression.

The calculated Michaelis–Menten constant of formate conversion (K_s) for cells of strain CP80 was 31.2 ± 7.3 μM and the calculated maximum velocity of formate conversion (V_{max}) was 36.0 ± 5.0 nmol h^{-1} (Fig. 3B), which is roughly 2.5-fold higher than the observed maximum rate of formate mineralization (calculated without normalizing to C assimilated) by CP80 grown with 50 μM formate (14.9 ± 4.9 nmol h^{-1}). Together, these results suggest a reduced efficiency for CP80 to utilize formate at low concentrations.

Genomic characterization of *Thermoproteus* sp. CP80

Paired-end Illumina MiSeq libraries were generated from genomic DNA, assembled and annotated to provide additional insight into formate, H_2/CO_2 and S_8° metabolism in strain CP80. Assembly of the CP80 genome yielded 187 contigs with a predicted genome size of 2.35 mega base pairs and a predicted GC content of 46.5%. Based on sequence homology, the partial genome sequence of CP80 predicts genes encoding a single putative 'O'-type FDH which consists of homologs of the alpha, beta and gamma, subunits of the FDH-O complex organized in an apparent operon (Table S1, Fig. S3, Supporting Information). The presence of a twin-arginine motif in the alpha subunit indicates that it is targeted for transport across the membrane. The alpha, beta and gamma subunit encoding genes exhibit 94%, 92% and 79% sequence identities to FDH-O homologs in *T. uzoniensis* 768-20.

A single, trimeric [NiFe]-hydrogenase complex was predicted in the genome of *Thermoproteus* sp. CP80 based on homology of a suite of genes. The large subunit of this complex exhibits 97% sequence identity to the large subunit of a group 1, uptake nickel-iron ([NiFe])-hydrogenase in *T. uzoniensis* 768-20. Two genes located immediately upstream of the large subunit are homologous to the small subunit (95% sequence identities) and the cytochrome *b* containing subunit (91% sequence identities) in the genome of *T. uzoniensis* 768-20. These genes are also organized as an apparent operon (Fig. S4, Supporting Information), and the encoded proteins are targeted for transport across the membrane by a twin-arginine motif present in the small subunit (Vignais, Billoud and Meyer 2001).

In addition to genes encoding a putative FDH and a [NiFe]-hydrogenase, genes encoding homologs of a multimeric sulfur reductase (Sre) complex putatively involved in S_8° reduction (Mardanov *et al.* 2010) were predicted based on homology. The genes encoding the three subunits (A, B, C) that comprise this complex were colocalized and exhibited 90%, 94% and 88% identity to SreABC subunits present in the genome of *T. uzoniensis* 768-20. SreA contains an N-terminal twin-arginine motif indicating that it is likely oriented on the outer side of the membrane. Additional genes encoding proteins involved in energy conservation identified in the genome of CP80 include a multimeric V-type ATP synthase complex as well as a number of proteins that are likely to be involved in the electron transport chain including homologs of NADH dehydrogenase and NADH-ubiquinone oxidoreductase (Table S1, Supporting Information).

A complement of gene homologs encoding the majority of enzymes involved in the dicarboxylate/4-hydroxybutyrate pathway of CO_2 fixation was also identified in the CP80 genome based on homology (Table 1, Fig. S5, Supporting Information). The presence of genes encoding homologs of all but three enzymes in this pathway in CP80 is consistent with the known distribution of the pathway in the archaeal orders *Desulfurococcales* and *Thermoproteales*, including *Thermoproteus* spp. (Ramos-Vera, Berg and Fuchs 2009; Ramos-Vera *et al.* 2010).

DISCUSSION

Thermoproteus strain CP80, a facultative autotroph, was isolated from CP, a sulfur-rich, high-temperature (89°C) hydrothermal feature in YNP using formate as the electron donor and carbon source and S_8° as the electron acceptor. The partial 16S rRNA gene sequence from the genome of CP80, which exhibited 100% sequence identity with the numerically dominant archaeal 16S rRNA gene sequence obtained previously from CP sediments (Urschel *et al.* 2015), was 98.8% identical to that from *T. uzoniensis* 768-20, an S_8°-reducing, anaerobic heterotroph belonging to the crenarchaeal order *Thermoproteales* (Bonch-Osmolovskaya *et al.* 1990). CP80 couples formate oxidation to S_8° reduction at temperature and pH conditions similar to those present *in situ* (Fig. 2). To our knowledge, this the first report of coupling of formate oxidation with reduction of S_8° by a crenarchaeote.

Formate metabolism by CP80 ceased when the concentration of formate remaining in batch cultures initially approached 27 μM and, following amendment with an additional 50 μM formate, ceased again when it approached 60 μM (Fig. 1B). This indicates that formate transformation in these cultures is limited by factor(s) other than formate availability. One factor may be a buildup of sulfide during S_8°-dependent growth. Sulfide toxicity in microbes is well documented (Castenholz 1977; McCartney and Oleszkiewicz 1991; Reis *et al.* 1992; Russell 1992; Okabe *et al.* 1995; Nicholls *et al.* 2013) and may stem from inhibition of key enzymes, or a decrease in the membrane potential via diffusion of sulfide into the cytosol and subsequent deprotonation of uncharged (protonated) sulfide (H_2S). Since the pKa for the dissociation of H_2S to HS^- is 6.6 at 80°C (Amend and Shock 2001), the majority of sulfide produced during S_8°-dependent growth in medium with a pH of 4.0 would be in the protonated form, making it necessary for the cell to expend additional energy to prevent accumulation of protons from deprotonated H_2S in the cytosol. Consistent with this suggestion, sulfide accumulation in bulk medium has been shown to increase the doubling (generation) time of some hyperthermophilic microorganisms due to increased maintenance energy requirements (Okabe *et al.* 1995). In support of these past observations is evidence that amendment of CP80 cultures with increasing concentrations of sulfide suppresses the total amount of formate mineralized (Supplemental Results and Fig. S3C, Supporting Information).

When grown on $H_2/CO_2/S_8^\circ$, strain CP80 did not exhibit a slowing or cessation of C assimilation activity, or growth, despite a final maximum sulfide concentration that was more than 3-fold higher than that observed when CP80 was grown on formate/S_8° (Fig. 2). One possible explanation for this result is that the cessation of formate metabolism and the lower cell yields observed in formate-grown cultures of CP80 at high sulfide concentration are due to the combined (additive) toxicity of formate and sulfide, rather than the toxicity of sulfide alone. Indeed, the generation times of cultures of CP80 increased and the total amount of sulfide produced (proxy for S_8° reduction) decreased with increasing initial formate concentrations in cultivation medium (Fig. S3A andB, respectively, Supporting Information). Consistent with these observations, sulfate-reducing bacteria (SRB) grown with the organic acids butyrate, acetate and propionate were reported to be more than 2-fold more sensitive to increased sulfide concentrations and pH changes (which effect the protonation ratio of sulfide and organic acids), when compared to SRB grown on H_2/CO_2 (O'Flaherty *et al*. 1998).

The calculated Gibbs free energy for the formate/S_8° redox couple remained lower than the H_2/S° redox couple throughout the growth period (Fig. S2, Supporting Information), indicating that it should be preferred for energetic reasons. In support of this prediction, the mass of C assimilated per unit energy conserved (Table 2) by CP80 cells grown on $H_2/CO_2/S_8^\circ$ was an order of magnitude lower than that observed during growth on formate/S_8°, despite the fact that the amount of C assimilated per cell was not significantly different between the two growth conditions (Table 2). These results indicate that, in addition to the lower energy yield available from the oxidation of H_2 with S_8°, growth of CP80 on $H_2/CO_2/S_8^\circ$ is a less efficient, more energy-intensive process than growth on formate. This finding was corroborated by calculations of the amount of energy required to synthesize a cell under $H_2/CO_2/S_8^\circ$ and formate/S_8° conditions, which indicated that cellular synthesis under the former conditions was a factor of 5 less efficient than the latter conditions (Table 2). While normalizing cellular synthesis efficiencies to the amount of energy required to synthesize a cell is perhaps non-conventional relative to normalizing to energy required to synthesize a unit of biomass (Heijnen and Van Dijken 1992), we suggest that from an ecological perspective this metric is perhaps more inclusive since it provides an integrated assessment of energy metabolism and efficiency at the level of the entire cell. A similar approach was used to evaluate temperature adaptation in a psychrophilic thiosulfate oxidizing *Thiobacillus* strain (Harrold *et al*. 2016). Intriguingly, the amount of energy required to synthesize a bacterial *Thiobacillus* cell, as determined in Harrold *et al*. (2016), ranged from 2.3 to 7.7 μJ cell^{-1}, values which are similar to the values (0.5–2.5 μJ cell^{-1}) determined to synthesize an archaeal *Thermoproteus* CP80 cell. This may point to a universal energy quantum for synthesis of a microbial cell in laboratory grown cultures.

To further evaluate this possibility, we combined rates of C assimilation cell^{-1} with energetic calculations to calculate biomass yields during autotrophic growth with H_2 and heterotrophic growth with formate. The amount of carbon assimilated during autotrophic and heterotrophic growth in exponential phase cultures were 1.2 ± 0.37 and 0.56 ± 0.36 pg cell^{-1}, which are similar to measurements previously made on heterotrophically grown cells of *Escherichia coli* (Fagerbakke, Heldal and Norland 1996; Loferer-Krößbacher, Klima and Psenner 1998) and *Vibrio natriegens* (Fagerbakke, Heldal and Norland 1996). Normalizing these quantities to the amount of energy dissipated during synthesis of biomass as determined by thermodynamic calculations and taking into account error, we arrive at a range of 191–855 kJ g C^{-1} for heterotrophically grown cells and 980–20707 kJ g C^{-1} assimilated for autotrophically grown cells. Values for heterotrophically grown CP80 cells are close to those reported previously for a taxonomically diverse array of heterotrophs grown with a variety of carbon sources (9–175 kJ g C^{-1}), while those for autotrophically grown CP80 cells are similar to those reported previously for a taxonomically diverse array of autotrophs (70–385 kJ g C^{-1}) (Heijnen and Van Dijken 1992) and are consistent with the preferential use of formate by CP80 for bioenergetic reasons. Importantly, the values determined here for the thermoacidophilic strain CP80 are on the higher end of those reported previously for mesophilic strains (Heijnen and Van Dijken 1992) which may point to increased maintenance energy costs in extreme environments characterized by low pH and or high-temperature (McCollom and Amend 2005; Hoehler 2007).

The decreased efficiency of growth on H_2/CO_2, compared to that on organic acids, has been observed in other organisms. For example, *Acetobacterium woodii* (Peters, Janssen and Conrad 1998; Scholten and Conrad 2000) required 8.8-fold greater maintenance energy when grown on H_2/CO_2 when compared to growth on lactate. Moreover, *Pseudomonas oxalaticus* OXl grown on succinate as electron donor required 4.4- and 1.9-fold more ATP when grown on CO_2 when compared to growth with glucose and oxalate, respectively (Dijkhuizen, Wiersma and Harder 1977). A possible explanation for such observations was proposed by Ishaque, Donawa and Aleem (1971) in studies of *Pseudomonas saccharophila* (Ishaque, Donawa and Aleem 1971). Here, a lower ATP phosphorylation per unit O_2 consumed (P/O ratio) during autotrophic growth, as compared to heterotrophic growth, was interpreted to be an indicator of poor coupling of substrate oxidation to ATP phosphorylation in the electron transport system used during autotrophic growth. While strain CP80 was not grown with O_2, a similar phenomenon may be expected with other terminal electron acceptors (e.g. S_8°).

The decreased efficiency of coupling energy conservation to cell or biomass production in strain CP80 when grown with $H_2/CO_2/S_8^\circ$ strongly suggests that growth on formate/S_8° should be preferred over growth on $H_2/CO_2/S_8^\circ$. To further investigate this hypothesis, we determined the extent to which formate amendment suppresses CO_2 assimilation in cells of CP80 growing with H_2 and S_8° (Fig. 3A). CO_2 assimilation in cultures of CP80 was suppressed by 20 μM formate, which is the minimum concentration of formate that was previously determined to suppress CO_2 assimilation in sediments sampled from CP (Urschel *et al*. 2015). Additional experiments indicated that suppression was not due to formate toxicity, which occurred only at formate concentrations >200 μM (see Figs S3A and S3B, Supporting Information). Moreover, the measured K_s of formate conversion by CP80 in culture (31.2 ± 7.3 μM, Fig. 3B) is similar to the K_s for formate conversion determined previously for CP sediment-associated communities (36.9 μM) (Urschel *et al*. 2015). The observed similarity between kinetic properties of formate/S_8° grown CP80 cells in pure culture and the formate uptake kinetics exhibited by the natural microbial community in CP indicates that the environmental conditions influencing the use of formate in CP are likely similar to those in CP80 microcosms. Taken together, these results indicate that strain CP80 preferentially utilizes the more energetically favorable substrate formate over H_2 when both are available, is capable of metabolic switching between H_2/CO_2 and formate/S_8° metabolism over short periods of time, and may be an important driver of primary production and formate transformation in CP.

CONCLUSIONS

In conclusion, our results demonstrate that the hyperthermophilic crenarchaeote *Thermoproteus* strain CP80 is a facultative autotroph capable of conserving energy for growth and maintenance from the coupling of formate or H_2 oxidation to S_8° reduction. To our knowledge, this is the first demonstration of the coupling of formate oxidation to S_8° reduction in a hyperthermophilic crenarchaeote. The results of H_2/CO_2 growth experiments, combined with the observed suppression of CO_2 assimilation in CP80 in the presence of formate, demonstrate that CP80 is capable of switching its metabolism in response to the availability of more energetically favorable organic substrates. Partial sequencing and analysis of CP80's genome revealed the presence of putative genes that are consistent with this organism's ability to conserve energy from both formate and H_2/CO_2, using S_8° as sole electron acceptor, and to utilize formate or CO_2 as a carbon source (see Figs S4 and S5, Supporting Information, and associated discussion).

The remarkable similarity between the kinetic properties of formate utilization exhibited by CP80 in culture and those exhibited by the chemosynthetic community present in CP indicates that this organism is adapted to formate utilization in its native habitat where it likely plays a key role as a primary producer and heterotroph, depending on availability of carbon sources and electron donors. The ability of CP80 to utilize both formate and H_2/CO_2, when combined with the presence of putative homologs for FDH, [NiFe]-hydrogenase, Sre and enzymes of the dicarboxylate/4-hydroxybutyrate cycle in CP80 (Table 1, Figs S4 and S5, Supporting Information) and numerous previously characterized autotrophic and heterotrophic crenarchaeaotes (Fig. 4)

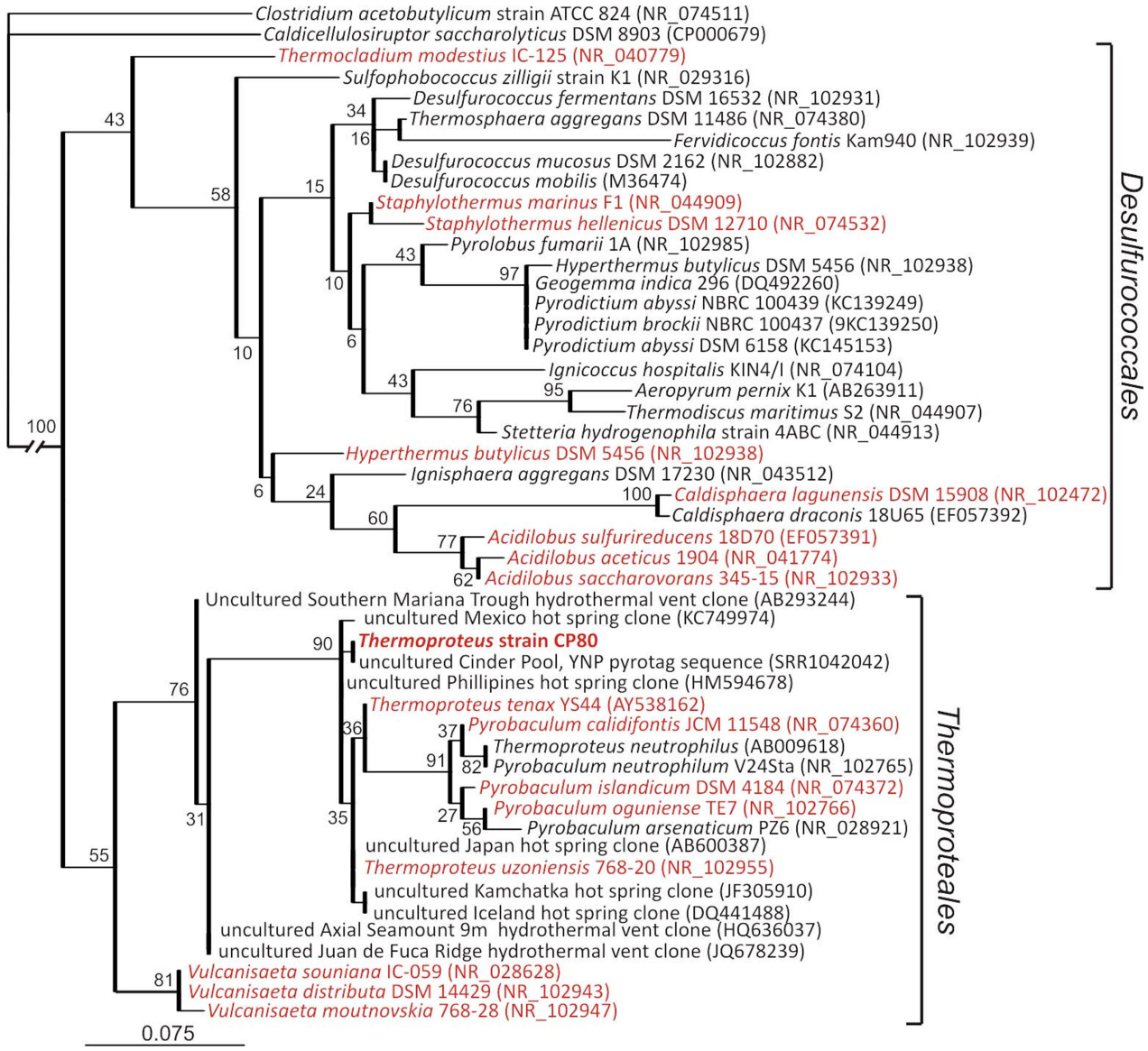

Figure 4. Maximum-likelihood (ML) phylogenetic reconstruction of partial archaeal 16S rRNA genes from cultivated and uncultivated organisms, including *Thermoproteus* strain CP80. Organisms with the demonstrated ability to reduce S_8° and which encode for homologs of FDH in their genomes are highlighted in red. Those taxa that are not denoted in red text either are not known to reduce S_8°, do not have an available genome sequence, or are from uncultivated lineages. Representative 16S rRNA gene sequences were compiled from the NCBI database using BLASTn with the 16S rRNA gene from strain CP80 as the query. Genes were aligned and subjected to evolutionary model prediction and ML phylogenetic reconstruction as described previously (Boyd *et al.* 2013). The phylogeny is based on an alignment of 240 positions and is rooted with bacterial 16S rRNA genes, as indicated. The hash was introduced to conserve space.

suggests that the ability to utilize and switch between formate and H_2/CO_2 as an energy and carbon source with S_8° as an electron acceptor is likely more widespread than previously thought.

SUPPLEMENTARY DATA

Supplementary data are available at FEMSEC online.

ACKNOWLEDGEMENTS

The authors wish to thank Christie Hendrix and Stacey Gunther from the YNP Center for the Resources for assistance in obtaining permits to perform this work.

FUNDING

This work was supported by the NSF Partnerships in International Research and Education award PIRE-0968421 (ESB). The NASA Astrobiology Institute is supported by NASA award NNA13AA94A (EER and ESB) and NNA15BB02A (ESB).

Conflict of interest. None declared.

REFERENCES

Amend JP, Rogers KL, Shock EL *et al.* Energetics of chemolithoautotrophy in the hydrothermal system of Vulcano Island, southern Italy. *Geobiology* 2003;**1**:37–58.

Amend JP, Shock EL. Energetics of overall metabolic reactions of thermophilic and hyperthermophilic Archaea and Bacteria. *FEMS Microbiol Rev* 2001;**25**:175–243.

Aziz RK, Bartels D, Best AA *et al.* The RAST Server: rapid annotations using subsystems technology. *BMC Genet* 2008;**9**:75.

Bolger AM, Lohse M, Usadel B. Trimmomatic: a flexible trimmer for Illumina sequence data. *Bioinformatics* 2014;**30**:2114–20.

Bonch-Osmolovskaya E, Miroshnichenko M, Kostrikina N *et al.* *Thermoproteus uzoniensis* sp. nov., a new extremely thermophilic archaebacterium from Kamchatka continental hot springs. *Arch Microbiol* 1990;**154**:556–9.

Boyd E, Hamilton T, Wang J *et al.* The role of tetraether lipid composition in the adaptation of thermophilic Archaea to acidity. *Front Microbiol* 2013;**4**:62.

Boyd ES, Jackson RA, Encarnacion G *et al.* Isolation, characterization, and ecology of sulfur-respiring Crenarchaea inhabiting acid-sulfate-chloride-containing geothermal springs in Yellowstone National Park. *Appl Environ Microb* 2007;**73**:6669–77.

Castenholz RW. The effect of sulfide on the blue-green algae of hot springs II. Yellowstone National Park. *Microbial Ecol* 1977;**3**:79–105.

Dick JM. Calculation of the relative metastabilities of proteins using the CHNOSZ software package. *Geochem T* 2008;**9**:10.

Dijkhuizen L, Wiersma M, Harder W. Energy production and growth of *Pseudomonas oxalaticus* OX1 on oxalate and formate. *Arch Microbiol* 1977;**115**:229–36.

Fagerbakke KM, Heldal M, Norland S. Content of carbon, nitrogen, oxygen, sulfur and phosphorus in native aquatic and cultured bacteria. *Aquat Microbiol Ecol* 1996;**10**:15–27.

Fischer F, Zillig W, Stetter K *et al.* Chemolithoautotrophic metabolism of anaerobic extremely thermophilic archaebacteria. *Nature* 1983;**301**:511–3.

Fogo JK, Popowsky M. Spectrophotometric determination of hydrogen sulfide. *Anal Chem* 1949;**21**:732–4.

Hamilton TL, Peters JW, Skidmore ML *et al.* Molecular evidence for an active endogenous microbiome beneath glacial ice. *ISME J* 2013;**7**:1402–12.

Harrold ZR, Skidmore ML, Hamilton TL *et al.* Aerobic and anaerobic thiosulfate oxidation by a cold-adapted, subglacial chemoautotroph. *Appl Environ Microb* 2016;**82**:1486–95.

Heijnen JJ, Van Dijken JP. In search of a thermodynamic description of biomass yields for the chemotrophic growth of microorganisms. *Biotechnol Bioeng* 1992;**39**:833–58.

Helgeson HC. Prediction of the thermodynamic properties of electrolytes at high pressures and temperatures. *Phys Chem Earth* 1981;**13**:133–77.

Hoehler TM. An energy balance concept for habitability. *Astrobiology* 2007;**7**:824–38.

Huber H, Burggraf S, Mayer T *et al.* *Ignicoccus* gen. nov., a novel genus of hyperthermophilic, chemolithoautotrophic Archaea, represented by two new species, *Ignicoccus islandicus* sp nov and *Ignicoccus pacificus* sp nov. *Int J Syst Evol Micr* 2000;**50**:2093–100.

Huber H, Gallenberger M, Jahn U *et al.* A dicarboxylate/4-hydroxybutyrate autotrophic carbon assimilation cycle in the hyperthermophilic Archaeum *Ignicoccus hospitalis*. *P Natl Acad Sci USA* 2008;**105**:7851–6.

Huber R, Kristjansson J, Stetter K. *Pyrobaculum* gen. nov., a new genus of neutrophilic, rod-shaped archaebacteria from continental solfataras growing optimally at 100°C. *Arch Microbiol* 1987;**149**:95–101.

Ishaque M, Donawa A, Aleem M. Oxidative phosphorylation in *Pseudomonas saccharophila* under autotrophic and heterotrophic growth conditions. *Biochem Bioph Res Co* 1971;**44**:245–51.

Loferer-Krößbacher M, Klima J, Psenner R. Determination of bacterial cell dry mass by transmission electron microscopy and densitometric image analysis. *Appl Environ Microb* 1998;**64**:688–94.

McCartney D, Oleszkiewicz J. Sulfide inhibition of anaerobic degradation of lactate and acetate. *Water Res* 1991;**25**:203–9.

McCollom TM, Amend JP. A thermodynamic assessment of energy requirements for biomass synthesis by chemolithoautotrophic micro-organisms in oxic and anoxic environments. *Geobiology* 2005;**3**:135–44.

Mardanov AV, Gumerov VM, Beletsky AV *et al.* Complete genome sequence of the thermoacidophilic crenarchaeon *Thermoproteus uzoniensis* 768-20. *J Bacteriol* 2011;**193**:3156–7.

Mardanov AV, Svetlitchnyi VA, Beletsky AV *et al.* The genome sequence of the crenarchaeon *Acidilobus saccharovorans* supports a new order, *Acidilobales*, and suggests an important ecological role in terrestrial acidic hot springs. *Appl Environ Microb* 2010;**76**:5652–7.

Nicholls P, Marshall DC, Cooper CE *et al.* Sulfide inhibition of and metabolism by cytochrome c oxidase. *Biochem Soc T* 2013;**41**:1312–6.

Nurk S, Bankevich A, Antipov D *et al.* Assembling single-cell genomes and mini-metagenomes from chimeric MDA products. *J Comp Biol* 2013;**20**:714–37.

O'Flaherty V, Mahony T, O'Kennedy R *et al.* Effect of pH on growth kinetics and sulphide toxicity thresholds of a range of methanogenic, syntrophic and sulphate-reducing bacteria. *Process Biochem* 1998;**33**:555–69.

Okabe S, Nielsen P, Jones W *et al.* Sulfide product inhibition of *Desulfovibrio desulfuricans* in batch and continuous cultures. *Water Res* 1995;**29**:571–8.

Peters V, Janssen P, Conrad R. Efficiency of hydrogen utilization during unitrophic and mixotrophic growth of *Acetobacterium woodii* on hydrogen and lactate in the chemostat. *FEMS Microbiol Ecol* 1998;**26**:317–24.

Plumb JJ, Haddad CM, Gibson JA *et al*. *Acidianus sulfidivorans* sp. nov., an extremely acidophilic, thermophilic archaeon isolated from a solfatara on Lihir Island, Papua New Guinea, and emendation of the genus description. *Int J Syst Evol Micr* 2007;**57**:1418–23.

Pronk JT, Meijer WM, Hazeu W *et al*. Growth of *Thiobacillus ferrooxidans* on formic acid. *Appl Environ Microb* 1991;**57**:2057–62.

Ramos-Vera WH, Berg IA, Fuchs G. Autotrophic carbon dioxide assimilation in *Thermoproteales* revisited. *J Bacteriol* 2009;**191**:4286–97.

Ramos-Vera WH, Labonté V, Weiss M *et al*. Regulation of autotrophic CO_2 fixation in the archaeon *Thermoproteus neutrophilus*. *J Bacteriol* 2010;**192**:5329–40.

Reis M, Almeida J, Lemos P *et al*. Effect of hydrogen sulfide on growth of sulfate reducing bacteria. *Biotechnol Bioeng* 1992;**40**:593–600.

Rogers K, Amend J. Archaeal diversity and geochemical energy yields in a geothermal well on Vulcano Island, Italy. *Geobiology* 2005;**3**:319–32.

Rogers KL, Amend JP. Energetics of potential heterotrophic metabolisms in the marine hydrothermal system of Vulcano Island, Italy. *Geochim Cosmochim Acta* 2006;**70**:6180–200.

Rogers KL, Amend JP, Gurrieri S. Temporal changes in fluid chemistry and energy profiles in the Vulcano island hydrothermal system. *Astrobiology* 2007;**7**:905–32.

Russell J. Another explanation for the toxicity of fermentation acids at low pH: anion accumulation versus uncoupling. *J Appl Bacteriol* 1992;**73**:363–70.

Sander R. Compilation of Henry's law constants, version 3.99. *Atmos Chem Phys* 2014;**14**:29615–30521.

Schäfer S, Barkowski C, Fuchs G. Carbon assimilation by the autotrophic thermophilic archaebacterium *Thermoproteus neutrophilus*. *Arch Microbiol* 1986;**146**:301–8.

Schäfer S, Gotz M, Eisenreich W *et al*. ^{13}C-NMR study of autotrophic CO_2 fixation in *Thermoproteus neutrophilus*. *Eur J Biochem* 1989a;**184**:151–6.

Schäfer S, Paalme T, Vilu R *et al*. ^{13}C-NMR study of acetate assimilation in *Thermoproteus neutrophilus*. *Eur J Biochem* 1989b;**186**:695–700.

Schloss PD, Westcott SL, Ryabin T *et al*. Introducing mothur: open-source, platform-independent, community-supported software for describing and comparing microbial communities. *Appl Environ Microb* 2009;**75**:7537–41.

Scholten JC, Conrad R. Energetics of syntrophic propionate oxidation in defined batch and chemostat cocultures. *Appl Environ Microb* 2000;**66**:2934–42.

Selig M, Schönheit P. Oxidation of organic compounds to CO_2 with sulfur or thiosulfate as electron acceptor in the anaerobic hyperthermophilic archaea *Thermoproteus tenax* and *Pyrobaculum islandicum* proceeds via the citric acid cycle. *Arch Microbiol* 1994;**162**:286–94.

Spear JR, Walker JJ, Pace NR. Hydrogen and primary productivity: inference of biogeochemistry from phylogeny in a geothermal ecosystem. In: Inskeep WP, McDermott TR (eds). *Geothermal Biology and Geochemistry in Yellowstone National Park*. Bozeman: Montana State University, 2005, 113–28.

Spear JR, Walker JJ, Pace NR. Microbial ecology and energetics in yellowstone hotsprings. *Yell Sci* 2006;**14**:17–24.

Team RC. *R: A Language and Environment for Statistical Computing*. Vienna, Austria: R Foundation for Statistical Computing, 2012.

Urschel MR, Kubo MD, Hoehler TM *et al*. Carbon source preference in chemosynthetic hot spring communities. *Appl Environ Microb* 2015;**81**:3834–47.

Vignais PM, Billoud B, Meyer J. Classification and phylogeny of hydrogenases. *FEMS Microbiol Rev* 2001;**25**:455–501.

White DE, Hutchinson RA, Keith TEC. *Geology and Remarkable Thermal Activity of Norris Geyser Basin*, Vol. 75. Wyoming: Yellowstone National Park, 1988, 1–84.

Windman T, Zolotova N, Schwandner F *et al*. Formate as an energy source for microbial metabolism in chemosynthetic zones of hydrothermal ecosystems. *Astrobiology* 2007;**7**:873–90.

Zillig W, Reysenbach AL. *Thermoproteus*. *Bergey's Manual of Systematics of Archaea and Bacteria*. Hoboken, NJ: John Wiley & Sons, Ltd., 2015.

Zillig W, Stetter K, Schäfer W *et al*. *Thermoproteales*: a novel type of extremely thermoacidophilic anaerobic archaebacteria isolated from Icelandic solfataras. *Zbl Bakt Mik Hyg I C* 1981;**2**:205–27.